Fluorescence Quenching Analysis of the Association and Dissociation of a Diarylheterocycle to Cyclooxygenase-1 and Cyclooxygenase-2: Dynamic Basis of Cyclooxygenase-2 Selectivity†

Cheryl A. Lanzo,‡ Jason Sutin,‡,§ Scott Rowlinson,‡ John Talley,|| and Lawrence J. Marnett*,‡

Departments of Biochemistry and Chemistry, Center in Molecular Toxicology, Vanderbilt-Ingram Cancer Center, Vanderbilt University School of Medicine, Nashville, Tennessee 37232, and Department of Inflammatory Disease Research, Searle Research and Development, St. Louis, Missouri 63198-0001

Received December 2, 1999; Revised Manuscript Received March 15, 2000

ABSTRACT: Cyclooxygenase-1 (COX-1) and cyclooxygenase-2 (COX-2) are the enzymes responsible for the biosynthesis of the precursor to the biologically active prostaglandins, prostacyclin, and thromboxane and are the molecular targets for nonsteroidal antiinflammatory drugs (NSAIDs). Selective COX-2 inhibitors are antiinflammatory and analgesic but lack gastrointestinal toxicity, an undesirable side effect attributed to COX-1 inhibition. Crystallographic analysis of selective COX inhibitors complexed with either isoform provides some information about the molecular determinants of selectivity but does not provide information about the dynamics of inhibitor association/dissociation. We employed rapid-mixing techniques and fluorescence quenching to monitor the association and dissociation of a selective COX-2 inhibitor to COX-1 or COX-2. The association of the fluorescent diaryloxazole, SC299, with both enzymes occurs in a time-dependent fashion. Its binding to COX-2 occurs in three kinetically distinct steps whereas its binding to COX-1 occurs in two steps. In contrast to the relatively rapid association of SC299 with both enzymes, its dissociation from COX-2 is quite slow and occurs over several hours whereas the dissociation from COX-1 is complete in less than 1 min. The selectivity of SC299 as a COX-2 inhibitor correlates to its relative rates of dissociation from the two COX isoforms. A model is proposed for diarylheterocycle binding to COX's that integrates these kinetic data with available structural information.

Cyclooxygenases (COX)[1] are heme-containing enzymes that catalyze the conversion of arachidonic acid to PGH_2, the immediate precursor to the biologically active prostaglandins, prostacyclin, and thromboxane (*1*, *2*). Two isoforms of COX are known that produce prostaglandins in different tissues with very specific roles (*3*). COX-1 generates prostaglandins that are important in gastric cytoprotection and platelet aggregation, whereas COX-2 generates prostaglandins involved in inflammation and hyperalgesia. Nonsteroidal antiiflammatory drugs (NSAIDs) inhibit both COX isoforms to varying extents, leading to beneficial antiinflammatory and analgesic effects as well as gastrointestinal and hematologic side effects (*4*). Selective COX-2 inhibitors retain the antiinflammatory and analgesic activities of NSAIDs without the undesired side effects (*5*−*7*).

The most extensively developed class of selective COX-2 inhibitors are diarylheterocycles that contain a sulfonamide or methyl sulfone in one of the pendant rings (*6*). Steady-state kinetic measurements indicate that these compounds bind reversibly to both COX-1 and COX-2 but, once bound to COX-2, the inhibitor−protein complex undergoes a slow transition to a form in which the inhibitor is more tightly bound (*8*). Thus, a two-step kinetic mechanism has been proposed to explain COX-2−inhibitor selectivity (eq 1).

$$E + I \underset{k_{-1}}{\overset{k_1}{\rightleftharpoons}} [E\cdot I] \xrightarrow{k_2} [E\cdot I]^* \qquad (1)$$

$$K_i = k_{-1}/k_1 \qquad k_{inact} = (k_{-1} + k_2)/k_1$$

Detailed kinetic analysis of inhibitor−COX association is complicated by the overlap of the time course for enzyme inhibition with the rapid time course for enzyme catalysis and autoinactivation. Thus, we have employed fluorescence quenching techniques to probe enzyme−inhibitor binding by exploiting the fact that heme is a powerful fluorescence quencher (*9*). Previously, we were able to estimate heme−inhibitor distances and conduct preliminary kinetic studies of enzyme−inhibitor association using a pair of COX-1 and COX-2-selective thiazoles (Figure 1) with fluorescence emission spectra that overlap the heme absorption spectrum.

† This work was supported by research and center grants from the National Institutes of Health (CA47479, ES00267, and CA68484) and a training grant to C.A.L. (ES07028). S.R. is the recipient of a Charles Martin Fellowship from the National Health and Medical Research Council of Australia.

* To whom correspondence should be addressed: (615)-343-7329 (phone); (615)-343-7534 (fax); marnett@toxicology.mc.vanderbilt.edu (e-mail).

‡ Vanderbilt University School of Medicine.

§ Current address: Laboratory for Fluorescence Dynamics, Department of Physics, University of Illinois, Urbana-Champaign, Urbana, IL 61801.

|| Searle Research and Development.

[1] Abbreviations: COX, cyclooxygenase [prostaglandin endoperoxide synthase, prostaglandin G/H synthase (EC 1.14.99.1)]; NSAID, nonsteroidal antiinflammatory drug; SC299, 4-(2-methyl-4-phenyl-5-oxazolyl)benzenesulfonamide.

10.1021/bi992761o CCC: $19.00
Published on Web 04/29/2000

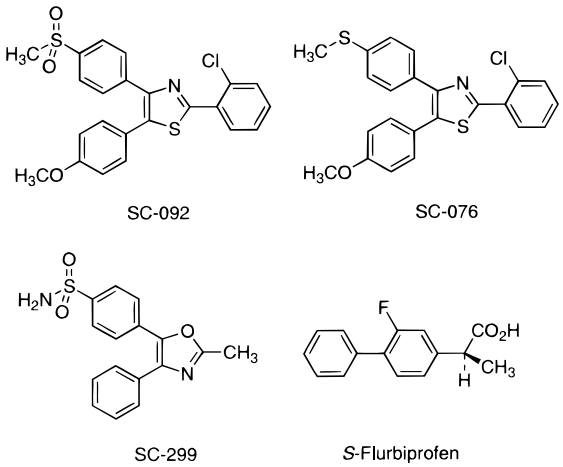

FIGURE 1: Chemical structures of selective COX inhibitors.

Fluorescence resonance energy transfer techniques provided distance estimates from SC076 to the heme of COX-1 of 20 Å and from SC092 to the heme of COX-2 of 18 Å (*9*). These values are consistent with the values determined from crystallographic analysis of COX-2 complexes with other diarylheterocycle inhibitors (*10*).

Recently, we have utilized a fluorescent oxazole, SC299, to measure the kinetics of association and dissociation with both COX isoforms. SC299 is a powerful, time-dependent inhibitor of COX-2 but a weak, reversible inhibitor of COX-1. The results of our stopped-flow kinetic experiments indicate that inhibitor binding to *both* COX isoforms is time dependent and occurs at comparable rates. However, a dramatic difference exists in the rate of dissociation of the inhibitor from the two enzymes that accounts for the selectivity of inhibition.

MATERIALS AND METHODS

Arachidonic acid was purchased from Nu Chek Prep (Elysian, MN). [1-^{14}C]Arachidonic acid (57 μCi/mmol) was purchased from NEN Dupont (Boston, MA). Hematin, CHAPS, Tris, and dimethyl sulfoxide were purchased from Sigma Chemical Co. (St. Louis, MO). (*S*)-Flurbiprofen was from the Upjohn Co. (Kalamazoo, MI). SC299 was synthesized as described (*11*). Octyl β-glucoside was purchased from Calbiochem (La Jolla, CA). Ram seminal vesicles were purchased from Oxford Biomedical Research, Inc. (Oxford, MI). Sheep COX-1 was purified from ram seminal vesicles as described (*12*). The isolated protein was 20% holoenzyme and had a specific activity of 10−20 μmol of arachidonic acid oxidized min^{-1} mg^{-1} after reconstitution with excess heme. Mouse COX-2 was expressed and purified as described (*13*). The isolated protein was 98% apoenzyme and had a specific activity of 6−10 μmol of arachidonic acid oxidized min^{-1} mg^{-1} after reconstitution with excess heme.

Equilibrium Binding of SC299 with COX. The fluorescence intensity of 2 μM SC299 titrated with 0.1−50 μM COX-1 and 0.1−10 μM COX-2 was measured in an ISS PC steady-state fluorometer. Excitation was at 331 nm and was polarized at the magic angle, 35.3°, to eliminate polarization bias. Emission was detected through 365, 370, and 375 nm long pass filters. Fluorescence intensities of the SC299 and COX mixtures were subtracted by the intensity of COX alone at each protein concentration.

Stopped-Flow Analysis of SC299 Binding to COX. Reactions were performed with an Applied Photophysics SX.18MV stopped-flow unit with a 100 μL cuvette and an auto stop assembly. For the on-rates, COX-1 or COX-2 (2 μM) was loaded in a separate syringe from SC299. For the off-rates, COX-1 or COX-2 (4 μM) was incubated with SC299 (0.5 μM) and loaded in a separate syringe from (*S*)-flurbiprofen. The conditions for the off-rates were developed to ensure that all of the inhibitor was bound at the beginning of the reaction. Extremely slow off-rates were measured in a Spex 1681 Fluorolog spectrofluorometer equipped with a 450 W xenon arc lamp to monitor dissociation over longer time scales. Excitation for all experiments was at 331 nm and was polarized with the magic angle set to 35.3° to eliminate polarization bias (*14*). Slits were set to 0.5 mm on the fluorometer for excitation and 2−4 mm on the stopped flow. Emission was detected through a 365 nm long pass filter for the stopped flow using a Hamamatsu emission photomultiplier with high voltage. For the off-rates with COX-2 in the fluorometer, emission was detected at 400 nm with slits set to 1 mm. All experiments were performed at 25 °C.

Data Analysis of SC299 with COX-1 and COX-2. The raw fluorescent intensity data were background subtracted by the mean of 2000 intensity measurements of the appropriate buffer or buffer with protein controls. The resulting kinetic traces of an entire titration experiment were globally analyzed for apparent rates by the Levenberg−Marquardt method of nonlinear least squares regression (*15*). The data sets for each individual concentration were given their own concentration-dependent rate and amplitude, and all of the concentrations were globally linked by one or two concentration-independent rates. The parameters were estimated by minimizing the total χ^2 of all of the fits at each concentration for the entire titration (*16*). The χ^2 was weighted by the error of the measured intensity at each point. The intensity error was estimated by the standard deviation of 2000 measurements of the fluorescence of SC299 alone at various concentrations for the different digitizer range settings used.

The uniqueness of the recovered parameters was established by rigorous confidence analysis of the global rates. A χ^2 curve was generated for each rate by optimizing all of the other parameters while holding the rate at various constant values. The standard errors associated with the recovered rates were determined from the χ^2 curves using the *F*-test at the 67% confidence limit.

Measurement of Heme Stoichiometry. The amount of heme bound to a specific enzyme preparation was measured by absorbance at 410 nm (ϵ = 123 000 M^{-1} cm^{-1}) (*17*). Excess heme was added to COX and allowed to equilibrate for 15 min on ice. Unbound heme was removed by gel filtration.

Kinetics of Inhibition As Determined by Thin-Layer Chromatography. The inhibition of cyclooxygenase activity of ovine COX-1 and murine COX-2 was measured by thin-layer chromatography. Standard reaction mixtures (200 μL) contained 300 nM COX-2, 500 μM phenol in 0.1 M Tris-HCl, pH 8.0, and the following inhibitor concentrations: 25 nM, 50 nM, 100 nM, 200 nM, or 1 μM SC299. Prior to the addition of inhibitor or [1-^{14}C]arachidonic acid, COX was reconstituted with 1 equiv of Fe-PPIX for 5 min. The preincubation time with inhibitor was varied from 15 s, 30 s, and 1, 2, 3, 5, or 10 min before the addition of 50 μM [1-^{14}C]arachidonic acid. Reactions were terminated after

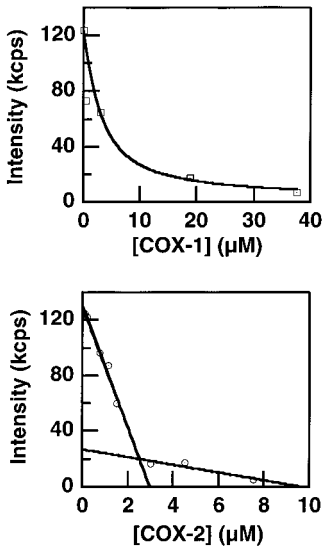

FIGURE 2: Equilibrium binding of SC299 with COX-1 and COX-2. SC299 (2 μM) was titrated with increasing concentrations of COX-1 (top) or COX-2 (bottom). Measurements were performed as described in Materials and Methods.

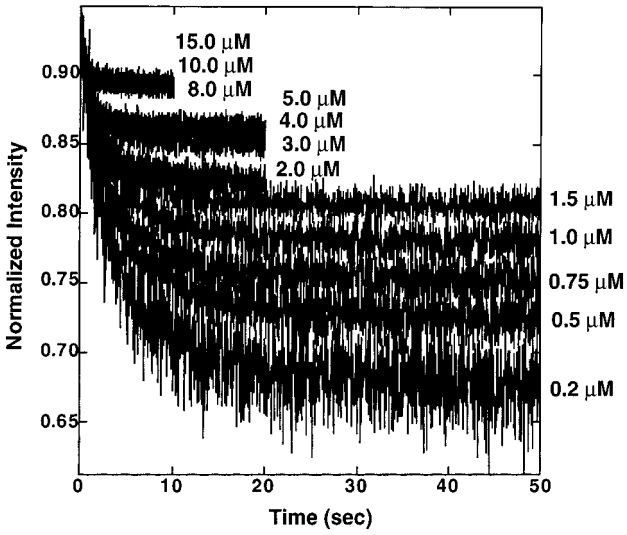

FIGURE 3: Association of SC299 with COX-1. COX-1 (2 μM) was rapidly mixed with SC299 (concentration is indicated beside each trace). The data were background subtracted and normalized to the intensity of free SC299 for each concentration. Stopped-flow measurements were made as described in Materials and Methods.

incubation with arachidonic acid for 30 s by solvent extraction with 200 μL of ethyl ether, methanol, and 1 M citric acid, pH 4.0 (30:4:1), containing 10 μg of butylated hydroxyanisole and 10 μg of unlabeled arachidonic acid. The organic layers were spotted onto silica gel plates, and the plates were developed with ethyl acetate/methylene chloride/glacial acetic acid (75:25:1) at 4 °C. Radiolabeled products were quantitated with a radioactivity scanner (Bioscan, Inc., Washington, DC).

RESULTS

SC299 is an oxazole that is highly selective for inhibition of COX-2 (*18*). Using a thin-layer chromatography assay, SC299 exhibited a K_i of 4 μM and a k_{inact} of 12.5 s^{-1} for mouse COX-2 but did not inhibit sheep COX-1 at concentrations as high as 1 mM. SC299 is fluorescent with a λ_{max} for emission of 406 nm and λ_{max} for excitation of 331 nm. The emission of SC299 overlaps the absorbance of the heme of COX, enabling fluorescence quenching techniques to be used to monitor the association and dissociation with COX-1 and COX-2 (*9*).

Equilibrium Binding Titration of SC299 with COX Measured by Fluorescence Quenching. To establish that COX-1 and COX-2 interacted with and quenched SC299 and to determine the K_D's of the interaction, we performed equilibrium binding studies with SC299 and both isoforms. SC299 exhibited increasing quenching with increasing concentrations of both COX-1 and COX-2 (Figure 2). Free heme or protein not containing heme did not quench SC299 fluorescence (data not shown). The binding of SC299 to COX-1 was described by a single species binding model where all of the bound states of SC299 were fit as a single bound state with an effective quantum yield representing the average of the quantum yields of the bound states populated at equilibrium. The resulting equilibrium K_D was 2 μM, and the effective intensity of the bound state of SC299 was 0.7% that of free SC299. COX-2 exhibited binding consistent with a K_D in the range of nanomolar or lower. Since the concentration of SC299 used was much higher than the K_D, a K_D could not be determined for the COX-2 titration. The stoichiometry of SC299 binding with COX-2 was determined to be approximately 1:1. At 10 μM COX-2, the intensity of SC299 was 4% that of free SC299.

Association of SC299 with COX-1. We monitored the fluorescence of increasing concentrations of SC299 following incubation with a single concentration of COX-1 (2 μM). Fluorescence was rapidly quenched at all SC299 concentrations, but the percentage of total fluorescence quenched decreased at higher concentrations of inhibitor due to the presence of increasing unbound inhibitor. The maximal extent of quenching was 35% at the lowest SC299 concentration. Decay curves, normalized to the fluorescence of free inhibitor at each concentration, are displayed in Figure 3. Association at all concentrations of SC299 was complete within 20 s as judged by maximal fluorescence quenching. For all concentrations of SC299, there was a small amount of quenching (5−10%) that occurred in the dead time of the instrument (not shown).

Global analysis of the apparent rates of association determined that each on-rate was best described by two exponentials. The data were fit to the following equation as described in Materials and Methods:

$$I(t) = A_0 + A_1 e^{-k_1 t} + A_2 e^{-k_2 t}$$

where $I(t)$ is the total intensity at time t, A_0 is the amplitude associated with free SC299, A_1 is the amplitude associated with the rate constant k_1, and A_2 is the amplitude associated with the rate constant k_2.

The rate constant, k_1, increased with SC299 concentration from 0.5 to 2.5 s^{-1}, and the resulting rate coefficient was 1.5×10^5 M^{-1} s^{-1}. The concentration-independent rate constant, k_2, was 0.14 s^{-1}. The goodness of fit as determined by χ^2 was 1.001 for the global fits (Table 1). Alternate models were tested to fit the data but resulted in poorer fits.

Association of SC299 with COX-2. Figure 4 displays the normalized decay curves of varying concentrations of SC299 incubated with a single concentration of COX-2 (2 μM).

Table 1: Rate Constants for the Association of COX-1 and COX-2 with SC299

reaction	k_1[a]	k_2[b]	k_3[b]	χ^2
on-rates COX-1 + SC299	1.5	0.14	na[c]	1.001
on-rates COX-2 + SC299	1.2	0.07	0.3	0.99

[a] k_1 is in units of $\times 10^5$ M^{-1} s^{-1}. [b] k_2 and k_3 correspond to intramolecular events. The order of the intramolecular event cannot be assigned at this time. Rate constants are expressed in units of s^{-1}. [c] na = not applicable.

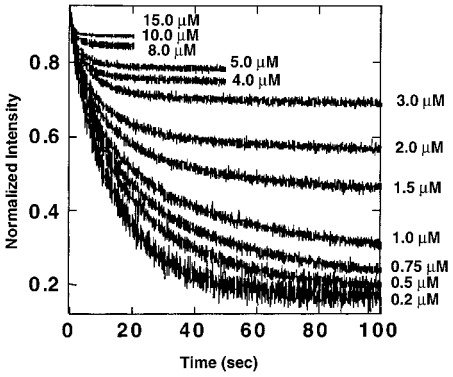

FIGURE 4: Association of SC299 with COX-2. COX-2 (2 μM) was rapidly mixed with SC299 (concentration is indicated beside each trace). The data were background subtracted and normalized to the intensity of free SC299 for each concentration. Stopped-flow measurements were made as described in Materials and Methods.

Association of SC299 with COX-2 was slower than the association with COX-1 but was complete within 80 s. Similar to COX-1, there was a small amount of quenching (5−10%) that occurred in the dead time of the instrument for all SC299 concentrations (not shown).

Global analysis of the apparent rates of SC299 fluorescence quenching by COX-2 revealed that the decay curves were described by three exponentials:

$$I(t) = A_0 + A_1 e^{-k_1 t} + A_2 e^{-k_2 t} + A_3 e^{-k_3 t}$$

To adequately fit the on-rates with COX-2, two of the three rate constants are zero order with respect to SC299 concentration, and the third rate constant is concentration dependent. The two concentration-independent rate constants are 0.07 s^{-1} and 0.3 s^{-1}. The concentration-dependent rate constant was invariant at 0.02 s^{-1} from SC299 concentrations up to 2 μM and then increased to 1.5 s^{-1} with a resulting rate coefficient of 1.2×10^5 M^{-1} s^{-1}. The χ^2 for the fits was 0.99 (Table 1).

Dissociation of SC299 from COX-1. To measure the dissociation of SC299 in real time, we prebound SC299 (0.5 μM) with COX-1 (4 μM) and then added a large excess of (*S*)-flurbiprofen. As SC299 was released from the enzyme, it was replaced by the nonfluorescent (*S*)-flurbiprofen, thereby regenerating fluorescence due to free inhibitor. An 8-fold excess of COX-1 was prebound to SC299 to ensure that all of the SC299 was associated with protein. Following addition of (*S*)-flurbiprofen, SC299 dissociated within 30 s (Figure 5). Several concentrations of (*S*)-flurbiprofen were used for competition and resulted in identical dissociation curves, indicating that the binding of (*S*)-flurbiprofen was not rate limiting for the reappearance of fluorescence (data not shown). In addition, COX-1 prebound to varying

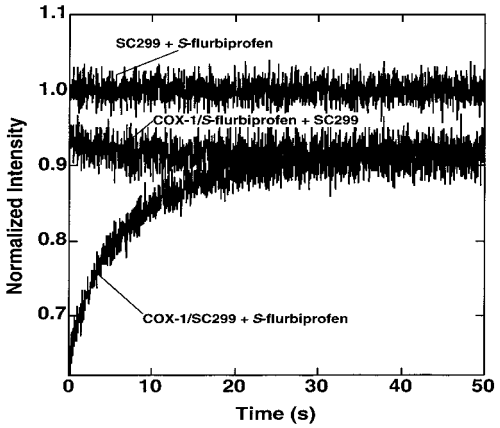

FIGURE 5: Competition of SC299 from COX-1 by (*S*)-flurbiprofen and of (*S*)-flurbiprofen from COX-1 by SC299. COX-1 (4 μM) was prebound to 0.5 μM SC299 or 100 μM (*S*)-flurbiprofen. The SC299 prebound complex was rapidly mixed with 100 μM (*S*)-flurbiprofen. The (*S*)-flurbiprofen prebound complex was rapidly mixed with 0.5 μM SC299. Controls include the preloaded complexes alone and 0.5 μM SC299 in the presence of 100 μM (*S*)-flurbiprofen but in the absence of enzyme. The resulting data were background subtracted and normalized to the intensity of free SC299 alone. Data were collected as described in Materials and Methods.

Table 2: Rate Constants for the Dissociation of SC299 from COX-1 and COX-2

reaction	k_{-1} (s^{-1})	k_{-2} (s^{-1})
off-rates COX-1:SC299 competed with *S*-flurbiprofen	0.1 (69%)[a]	0.36 (31%)[a]
off-rates COX-2:SC299 competed with *S*-flurbiprofen	2.5×10^{-4}	na[b]

[a] The amplitudes associated with each rate. The order of k_{-1} and k_{-2} cannot be assigned at this time. [b] na = not applicable.

concentrations of SC299 and then incubated with (*S*)-flurbiprofen resulted in superimposable dissociation curves, indicating that SC299 was occupying the same sites once bound to COX-1 independent of the concentration of SC299 (data not shown). Fits to the dissociation of SC299 from COX-1 demonstrated that the off-rate was multiexponential and was described by dissociation rate constants of 0.1 s^{-1} (69% amplitude) and 0.36 s^{-1} (31% amplitude) (Table 2).

The fluorescence of SC299 released from COX-1 did not return to that of an equal concentration of free inhibitor in the absence of protein (refer to Figure 5). If the remaining fluorescence quenching was due to SC299 bound at a competitive site or in rapid equilibrium with (*S*)-flurbiprofen, then a vast excess of (*S*)-flurbiprofen should return the fluorescence intensity to that of free SC299. Therefore, we measured the reappearance of fluorescence in the presence of a 10 000-fold excess of (*S*)-flurbiprofen. The fluorescence did not return to that of the free inhibitor (data not shown), which suggests that SC299 occupies an alternate binding site on COX-1 that does not compete with (*S*)-flurbiprofen and results in a small amount of quenching.

To further determine if a noncompetitive site for SC299 binding existed, a competition experiment was designed in which a 25-fold excess of (*S*)-flurbiprofen (100 μM) was preincubated with COX-1 (4 μM) and then mixed with 0.5 μM SC299. The results demonstrated a fast diffusion-limited association of SC299 with COX-1 even in the presence of (*S*)-flurbiprofen (Figure 5). Furthermore, the extent of

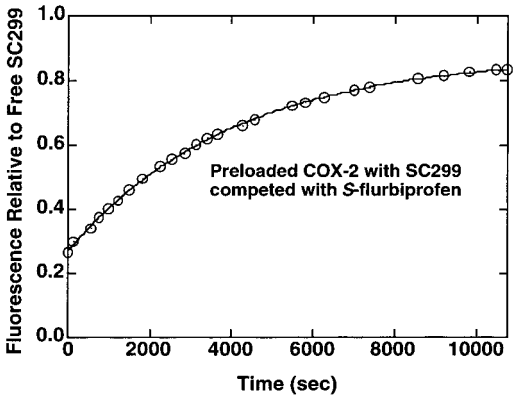

FIGURE 6: Competition of SC299 from COX-2 by (*S*)-flurbiprofen. COX-2 (4 μM) was prebound with 0.5 μM SC299 and mixed with 400 μM (*S*)-flurbiprofen. Data were background subtracted and normalized to the intensity of free SC299. Data were collected as described in Materials and Methods.

quenching matched the extent of quenching remaining after dissociation of SC299 from COX-1 (Figure 4) competed with (*S*)-flurbiprofen. These results strongly suggest the existence of a separate site for SC299 binding on COX-1 that is not competitive with (*S*)-flurbiprofen.

Dissociation of SC299 from COX-2. Similar experiments were performed to monitor the dissociation of SC299 from COX-2. There was no recovery of fluorescence intensity on the time scale in which total release was observed from COX-1. To measure an apparently much slower rate, the competition experiment was performed in a steady-state fluorometer. The release of SC299 occurred very slowly and required approximately 3 h to approach completion (Figure 6). Several (*S*)-flurbiprofen concentrations were used to compete with SC299 for COX-2 and resulted in identical dissociation curves (data not shown). The rate of dissociation of SC299 from COX-2 fit to a single exponential with a rate coefficient of 2.5×10^{-4} s^{-1}.

As with COX-1, a small amount of quenching remained after (*S*)-flurbiprofen competition of SC299 prebound to COX-2. An analogous experiment to the one described for COX-1 was performed with COX-2 prebound to (*S*)-flurbiprofen and mixed with SC299. A similar rapid but slight quenching of fluorescence was observed in the dead time of the instrument, suggesting the existence of a binding site for SC299 on COX-2 that is noncompetitive with (*S*)-flurbiprofen (data not shown).

DISCUSSION

Fluorescence quenching is an excellent technique for measuring the kinetics of association of small molecules with proteins. It is particularly useful in studies of heme proteins because the heme prosthetic group is a powerful fluorescence quencher. As fluorescent ligands move closer to the heme group, their fluorescence intensity decreases in a manner that is sensitive to the distance from the heme and the orientation of the fluorescence dipole of the ligand relative to the plane of the heme. We have previously used fluorescence resonance energy transfer in conjunction with molecular modeling to estimate the positions of the selective diarylthiazole inhibitors, SC076 and SC-092, bound to COX-1 and COX-2, respectively (*9*). The accuracy of the calculated distances was verified by comparison of the model for the SC092−COX-2 complex to the crystal structure of a complex between COX-2 and a related diarylheterocycle, SC-566 (*10*). No crystal structures have been reported for complexes of a diarylheterocycle with COX-1 so our model of SC-076 bound to COX-1 is the only currently available structure of a diarylheterocycle with COX-1.

Despite the high selectivity of SC-299 for COX-2, it binds rapidly to COX-1, as judged by the time course of fluorescence quenching following stopped-flow addition to the enzyme. The results indicate that the association of SC-299 with COX-1 and COX-2 occurs at similar rates over a period of about 30−120 s. However, SC-299 binds a little more quickly to COX-1 than it does to COX-2. In addition, by comparison of the steady-state intensities of SC299 under conditions in which all of the SC299 was bound to either COX-1 or COX-2, high fluorescence quenching was exhibited by both isoforms, indicating that SC299 travels to similar positions very deep in both COX-1 and COX-2.

The first step in binding is a bimolecular event dependent on enzyme and inhibitor concentrations that occurs with similar rate coefficients for both isoforms. After the initial association, the subsequent events are different for COX-1 and COX-2. In COX-1 a single unimolecular step takes the inhibitor deep into the enzyme. For simplicity of analysis, this step was considered to reflect only enzyme−inhibitor association although, given the rate coefficient for dissociation, it is likely that it represents an approach to equilibrium. In COX-2 the inhibitor reaches a similar depth inside the enzyme but requires two unimolecular events to complete. Thus, the major difference in binding to the two enzymes is that a third unimolecular event occurs in binding to COX-2.

Although there are clear-cut differences in the kinetics of association of SC299 with COX-1 and COX-2, the overall differences in the rates of association are too small to account for the selectivity of COX-2 inhibition. Thus, we investigated the dissociation of SC299 from COX-1 and COX-2 by monitoring the reappearance of fluorescence as the inhibitor diffused from the active site. These incubations were conducted in the presence of a large excess of the nonfluorescent inhibitor, flurbiprofen, to prevent reassociation of SC299 once it departed the active site. SC299 spontaneously dissociated from COX-1 in a two-step process that was complete within 30 s. In contrast, SC299 dissociated from COX-2 in a single-step process that required hours to complete. Comparison of the rate coefficients for dissociation indicated that release of SC299 from COX-2 was approximately 4000- or 1500-fold slower than from COX-1, depending on which first-order rate coefficient for dissociation from COX-1 is compared. Even with the caveat that these are not microscopic rate coefficients, it is clear that there is a reasonable correlation between the relative rates of dissociation and the selectivity for isoenzyme inhibition by SC299. Thus, the selectivity for inhibition of COX-2 by SC299 is determined by its very slow rate of dissociation.

These findings are consistent with previous reports from several laboratories that diarylheterocycles associate rapidly and reversibly with both COX isoforms and then undergo a slow transition that leads to a more tightly bound inhibitor in the selected isoform (*8*, *19*−*21*). The formation of the tightly bound complex accounts for the selectivity of inhibition for either form of the enzyme. The overall association of inhibitor with enzyme is usually depicted as

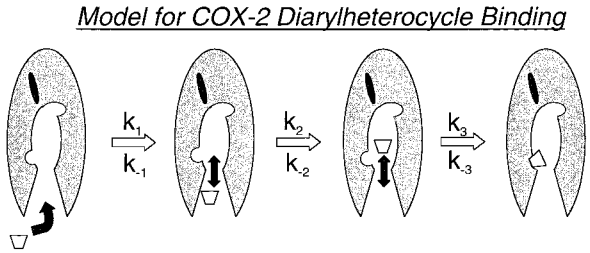

FIGURE 7: Three-step model of SC299 binding to COX-2. SC299 binds in the lobby region in the first step, moves past the constriction comprised of Arg120, Tyr355, and Glu524 in the second step, and then inserts into the side pocket bordered by Val523 in the third step. Insertion into the side pocket accounts for the stability of SC299 binding and the stability of inhibition.

a two-step process (eq 1) (*8*, *22*). However, using both equilibrium binding and pre-steady-state kinetic fluorescence quenching, we are able to observe that both isoforms bind the inhibitor deeply in a time-dependent manner. In COX-2, there is an additional step that occurs moderately quickly but leads to highly stabilized binding. This third step and the tight binding it generates accounts for the selectivity of inhibition of COX-2 by SC299.

COX-1 and COX-2 from various species are approximately 60% identical in sequence, and inspection of the crystal structures of both proteins reveals that their cyclooxygenase active sites are highly homologous (*10*, *23*−*27*). This similarity aids in the development of a structural model to explain the kinetic differences in binding and dissociation of SC299 with the two enzymes (Figure 7). The first two steps in inhibitor binding are very similar in rate and order (bimolecular and then unimolecular) and likely result from similar molecular movements in the active site channel. The bimolecular event represents the initial association of enzyme and inhibitor whereas the unimolecular event represents further movement up the channel. These movements likely occur in the broad opening, which we term the lobby, that leads from the membrane-binding domain to the constriction that separates the lobby from the upper part of the channel, which is the cyclooxygenase active site. We propose that initial inhibitor binding occurs in the lobby, and then the inhibitor moves past the constriction to the cyclooxygenase active site. The region from the lobby to the constriction is very similar in structure, and although there are differences in individual residues, none of them have been shown to contribute to inhibitor selectivity.

The major structural difference that does contribute to the isoform selectivity of diarylheterocycles is at position of 523 of COX-1 (509 of COX-2) (*28*−*30*). The Ile residue in COX-1 blocks access to a side pocket off the main cyclooxygenase channel whereas the Val residue at this position in COX-2 permits access to the side pocket (*27*). The sulfonamide or sulfone moiety of selective COX-2 inhibitors inserts into this side pocket and forms a stable complex that is responsible for selective inhibition (*10*). Mutation of the Val residue at position 509 of COX-2 to Ile renders the mutant protein resistant to time-dependent inhibition by diarylheterocycles (*28*, *30*). It is attractive to invoke movements in and out of this side pocket as the cause for the third step of SC299 binding to COX-2, which results in very slow off-rates. According to this model, SC299 passes the constriction into the cyclooxygenase active site in both proteins so it may be located at similar distances from the heme in each case. However, as the sulfonamide of the inhibitor inserts into the side pocket of COX-2, a specific interaction occurs leading to tight binding. This interaction does not occur on COX-1.

An important corollary of this model is that the second event responsible for fluorescence quenching in both enzymes represents the opening and closing of the constriction separating the lobby from the active site. This occurs with a rate coefficient of approximately 0.1 s^{-1}. An alternate model would have SC299 binding in the lobby and moving to a position underneath the constriction in the second step. The inhibitor would only pass into the cyclooxygenase active site in COX-2, which would result in the third step in fluorescence quenching. We believe this model is less attractive because of the structural similarity of the lobbies of the two COX enzymes. It is not clear how the protein structural changes above the constriction that are responsible for COX-2 selectivity could influence the rate of inhibitor movement through the constriction. Furthermore, the similarity in the extent of fluorescence quenching by COX-1 and COX-2 when all of the SC299 is bound suggests it is bound at a similar distance from the heme in both proteins. Our earlier modeling studies and the crystallographic analysis of a COX-2−SC558 complex suggest that this distance is approximately 20 Å, which places the bound inhibitor above the constriction that separates the lobby from the cyclooxygenase active site (*9*, *10*).

Finally, our results suggest that an alternate binding site exists for SC299 on COX-1 and COX-2 that is not competitive with (*S*)-flurbiprofen. The association of SC299 at this noncompetitive site occurs within the mixing time of the instrument and results in 5−10% quenching of fluorescence. Similarly, for the on-rate experiments, a small 5−10% quench occurs at a diffusion-controlled rate. Because this site is noncompetitive with (*S*)-flurbiprofen and since it is known that (*S*)-flurbiprofen binds in the cyclooxygenase active site (*10*, *26*), we do not believe that the noncompetitive site is in the cyclooxygenase active site. The noncompetitive site may represent a binding event not resulting in inhibition so it may not be pharmacologically relevant.

The slow, tight-binding model originally proposed by Rome and Lands has provided a useful paradigm with which to describe the interaction of inhibitors with COX (*22*). This two-step model of association is based on the kinetics of inhibition rather than real time measurements of binding. Inhibition studies are limited in their resolution by the similarity of the time courses for time-dependent inhibition and cyclooxygenase activity. This overlap makes it very difficult to dissect multiple inhibitory events that occur at similar rates. Our results demonstrate that association of selective inhibitors with COX isoforms is more complex than the two-step model. For example, SC299, a selective COX-2 inhibitor, rapidly associates and dissociates with COX-1 without resulting in a tightly bound inhibitor−enzyme complex. The similarities in the association and dissociation rates of the COX-1−SC299 complex account for the poor ability of SC299 to inhibit COX-1. However, even this rapidly reversible interaction of SC299 with COX-1 occurs in two steps, which does not adhere to the simple kinetic model for inhibition. The deviation from the slow, tight-binding model is more dramatic for COX-2 in that the

association occurs in three steps—two that are similar to COX-1 and a third step that results in an essentially irreversibly inhibited enzyme. This third event represents the establishment of an interaction with COX-2 not available to the inhibitor on COX-1. This interaction results in a tightly bound COX-2−SC299 complex in which the off-rate governs isoform selectivity.

The present study establishes parameters for the use of fluorescence quenching to monitor association of selective inhibitors with their respective COX targets. This allows us to measure dynamic events associated with the real time binding of these fluorescent molecules using stopped-flow techniques. The fluorescence data complement the available crystallographic data in that the crystal structures present a static picture of enzyme−inhibitor association but do not provide information about the kinetics of association and their dependence on individual residues in the substrate access channel. There are multiple opportunities for the use of fluorescence quenching to monitor dynamics of inhibitor−enzyme association, and we provide here preliminary data demonstrating the utility of this approach. Kinetic analysis of COX-2 mutants that render it similar to COX-1 with respect to inhibitor specificity will provide a test for our model of enzyme−inhibitor interactions.

ACKNOWLEDGMENT

We are grateful to D. Denson for assistance in protein preparation.

REFERENCES

1. Smith, W. L., Garavito, R. M., and DeWitt, D. L. (1996) *J. Biol. Chem. 271*, 33157−33160.
2. Marnett, L. J., Rowlinson, S. W., Goodwin, D. C., Kalgutkar, A. S., and Lanzo, C. A. (1999) *J. Biol. Chem. 274*, 22903−22906.
3. Vane, J. R., Bakhle, Y. S., and Botting, R. M. (1998) *Annu. Rev. Pharmacol. Toxicol. 38*, 97−120.
4. Laneuville, O., Breuer, D. K., DeWitt, D. L., Hla, T., Funk, C. D., and Smith, W. L. (1994) *J. Pharmacol. Exp. Ther. 271*, 927−934.
5. Marnett, L. J., and Kalgutkar, A. S. (1999) *Trends Pharmacol. Sci. 20*, 465−469.
6. Talley, J. J. (1999) *Prog. Med. Chem. 36*, 201−234.
7. Prasit, P., and Riendeau, D. (1997) *Annu. Rep. Med. Chem. 32*, 211−220.
8. Copeland, R. A., Williams, J. M., Giannaras, J., Nurnberg, S., Covington, M., Pinto, D., Pick, S., and Trzaskos, J. M. (1994) *Proc. Natl. Acad. Sci. U.S.A. 91*, 11202−11206.
9. Lanzo, C. A., Beechem, J., Talley, J., and Marnett, L. J. (1998) *Biochemistry 37*, 217−226.
10. Kurumbail, R. G., Stevens, A. M., Gierse, J. K., McDonald, J. J., Stegeman, R. A., Pak, J. Y., Gildehaus, D., Miyashiro, J. M., Penning, T. D., Seibert, K., Isakson, P. C., and Stallings, W. C. (1996) *Nature 384*, 644−648.
11. van Es, T., and Backberg, O. G. (1963) *J. Chem. Soc.*, 1363−1370.
12. Marnett, L. J., Siedlik, P. H., Ochs, R. C., Pagels, W. D., Das, M., Honn, K. V., Warnock, R. H., Tainer, B. E., and Eling, T. E. (1984) *Mol. Pharmacol. 26*, 328−335.
13. Rowlinson, S. W., Crews, B. C., Lanzo, C. A., and Marnett, L. J. (1999) *J. Biol. Chem. 274*, 23305−23310.
14. Badea, M. G., and Brand, L. (1979) *Methods Enzymol. 61*, 378−425.
15. Press, W., Teulolsky, S., Vettering, W., and Flannery, B. (1994) *Numerical Recipes in C: The Art of Scientific Computing*, 2nd ed., Cambridge University Press, New York.
16. Bevington, P. R., and Robinson, D. K. (1992) *Data Reduction and Error Analysis for the Physical Sciences*, 2nd ed., McGraw-Hill, New York.
17. Kulmacz, R. J., and Lands, W. E. M. (1984) *J. Biol. Chem. 259*, 6358−6363.
18. Talley, J. J., Bertenshaw, S. R., Brown, D. L., Carter, J. S., Graneto, M. J., Koboldt, C. M., Masferrer, J. L., Norman, B. H., Rogier, D. J., Jr., Zweifel, B. S., and Seibert, K. (1999) *Med. Res. Rev. 19*, 199−208.
19. Houtzager, V., Ouellet, M., Falgueyret, J. P., Passmore, L. A., Bayly, C., and Percival, M. D. (1996) *Biochemistry 35*, 10974−10984.
20. Gierse, J. K., Koboldt, C. M., Walker, M. C., Seibert, K., and Isakson, P. C. (1999) *Biochem. J. 339*, 607−614.
21. Callan, O. H., So, O. Y., and Swinney, D. C. (1996) *J. Biol. Chem. 271*, 3548−3554.
22. Rome, L. H., and Lands, W. E. M. (1975) *Proc. Natl. Acad. Sci. U.S.A. 72*, 4863−4865.
23. DeWitt, D. L., and Smith, W. L. (1988) *Proc. Natl. Acad. Sci. U.S.A. 85*, 1412−1416.
24. Merlie, J. P., Fagan, D., Mudd, J., and Needleman, P. (1988) *J. Biol. Chem. 263*, 3550−3553.
25. Toh, H., Yokoyama, C., Tanabe, T., Yoshimoto, T., and Yamamoto, S. (1992) *Prostaglandins 44*, 291−315.
26. Picot, D., Loll, P. J., and Garavito, R. M. (1994) *Nature 367*, 243−249.
27. Luong, C., Miller, A., Barnett, J., Chow, J., Ramesha, C., and Browner, M. F. (1996) *Nat. Struct. Biol. 3*, 927−933.
28. Gierse, J. K., McDonald, J. J., Hauser, S. D., Rangwala, S. H., Koboldt, C. M., and Seibert, K. (1996) *J. Biol. Chem. 271*, 15810−15814.
29. Wong, E., Bayly, C., Waterman, H. L., Riendeau, D., and Mancini, J. A. (1997) *J. Biol. Chem. 272*, 9280−9286.
30. Guo, Q., Wang, L.-H., Ruan, K.-H., and Kulmacz, R. J. (1996) *J. Biol. Chem. 271*, 19134−19139.

BI992761O